Hydrol. Earth Syst. Sci. Discuss., 12, 5219–5250, 2015
www.hydrol-earth-syst-sci-discuss.net/12/5219/2015/
doi:10.5194/hessd-12-5219-2015

Hydrology and Earth System Sciences Discussions
Open Access

Long-term effects of climate and land cover change on freshwater provision in the tropical Andes

A. Molina[1,2], V. Vanacker[3,4], E. Brisson[1,5], D. Mora[2], and V. Balthazar[3]

[1] Department of Earth and Environmental Sciences, KU Leuven, Celestijnenlaan 200E, 3001 Heverlee, Belgium
[2] Programa para el Manejo del Agua y del Suelo (PROMAS), Universidad de Cuenca, Av. 12 de abril s/n, Cuenca, Ecuador
[3] Earth and Life Institute, Georges Lemaitre Centre for Earth and Climate Research, University of Louvain, 3 Place Louis Pasteur, 1348 Louvain-la-Neuve, Belgium
[4] Secretaria de Educación Superior, Ciencia, Tecnología e Innovación, Whymper E7-37 y Alpallana, Quito, Ecuador
[5] Institute for Atmospheric and Environmental Sciences, Goethe University Frankfurt, Altenhöferallee 1, 60438 Frankfurt, Germany

Received: 30 April 2015 – Accepted: 13 May 2015 – Published: 5 June 2015

Correspondence to: A. Molina (molina_armando@hotmail.com)

Published by Copernicus Publications on behalf of the European Geosciences Union.

Abstract

Andean headwater catchments play a pivotal role to supply fresh water for downstream water users. However, few long-term studies exist on the relative importance of climate change and direct anthropogenic perturbations on flow regimes. In this paper, we assess multi-decadal change in freshwater provision based on long time series (1974–2008) of hydrometeorological data and land cover reconstructions for a 282 km^2 catchment located in the tropical Andes. Three main land cover change trajectories can be distinguished: (1) rapid decline of native vegetation in montane forest and páramo ecosystems in $\sim 1/5$ or 20 % of the catchment area, (2) expansion of agricultural land by 14 % of the catchment area, (3) afforestation of 12 % of native páramo grasslands with exotic tree species in recent years. Given the strong temporal variability of precipitation and streamflow data related to El Niño–Southern Oscillation, we use empirical mode decomposition techniques to detrend the time series. The long-term increasing trend in rainfall is remarkably different from the observed changes in streamflow that exhibit a decreasing trend. Hence, observed changes in streamflow are not the result of long-term climate change but very likely result from direct anthropogenic disturbances after land cover change. Partial water budgets for montane cloud forest and páramo ecosystems suggest that the strongest changes in evaporative water losses are observed in páramo ecosystems, where progressive colonization and afforestation of high alpine grasslands leads to a strong increase in transpiration losses.

1 Introduction

Andean headwater catchments play a pivotal role to supply fresh water for downstream water users (Urrutia and Vuille, 2009; Roa-García et al., 2011). Although the ecosystems in the tropical Andes have been modified by anthropogenic disturbances for at least 7000 years (Bruhns, 1994), it is only since the early 20th century that natural habitats have undergone extensive transformation (White and Maldonado, 1991). The demand for agricultural land has led to an expansion of the agricultural frontier at the expense of natural ecosystems. The magnitude and intensity of land use change have increased rapidly from the second half of the 20th century, as result of demographic growth, socio-economic development, internal and external migration, and land reform programs (Vanacker et al., 2003).

A major concern for sustainable development in the tropical Andes is the increasing demand for freshwater ecosystem services (Harden, 2006; Ponette-Gonzalez et al., 2014). The rapid growth of various mega-cities located in the high Andes will further exacerbate the demand for water resources in the near future, from drinking water to water for sanitation, irrigation and agriculture, mining operations, and hydropower production. Changes in freshwater flow regimes are predicted to lead to future water scarcity (Bradley et al., 2006) as a result of the combined effect of climate change and variability (Bathurst et al., 2011; Urrutia and Vuille, 2009), and direct anthropogenic impact (Harden, 2006).

Both change and variability in local climatic conditions produce changes in hydrological conditions (Poveda and Mesa, 1997; Restrepo and Kjerfve, 2000). In the tropical Andes, the temporal variability of precipitation is strongly related to oceanic and atmospheric conditions over the Pacific Ocean and Amazon basin (Vuille et al., 2000; Marengo et al., 2004). The impact of El Niño–Southern Oscillation (ENSO) is clearly noticeable on the Western escarpment of the Andes in Ecuador and northern Peru (Tapley and Waylen, 1990; Rossel, 1997), and decreases with altitude as the steep, high-altitude topography of the Andean range creates distinct microclimates (Mora and Willems, 2012).

Direct anthropogenic impact resulting from land cover change is rapidly transforming the hydrological functioning of tropical Andean ecosystems (Vanacker et al., 2003; Farley et al., 2004; Molina et al., 2012). The hydrological response is diverse, as changes in vegetation affect various components of the hydrological cycle including evapotranspiration (Nosetto et al., 2005), infiltration (Molina et al., 2007) and surface runoff (Bathurst et al., 2011). The clearance of native forest for arable and grazing land induces rapid changes in soil physical properties reducing soil infiltration capacity (Bosch and Hewlett, 1982; Molina et al., 2007), and increasing surface runoff as a result of soil compaction and reduced evapotranspiration (Ruprecht and Schofield, 1989). As a consequence, the conversion of native forests to agricultural land often results in an increase of the annual water yield, but a reduction of the low flows (Bruijnzeel, 1990; Andréassian, 2004). In contrast, afforestation and/or reforestation of grasslands and arable lands lead to a reduction in soil moisture and total water yield as a result of greater canopy interception and evapotranspiration (Bruijnzeel, 2004; Scott et al., 2005; Farley et al., 2005; Buytaert et al., 2007).

In tropical Andean ecosystems characterised by large inter- and intra-annual variability in hydrometeorological conditions, little is known about the relative importance of climate change and direct anthropogenic perturbations on streamflow. At large spatial scale ($> 100\,\text{km}^2$), the patterns of land cover change are notoriously dynamic, both in space and time, and are commonly associated to climatic and altitudinal gradients. In this paper, we assess multi-decadal change in freshwater provision based on long time series of hydrometeorological data and land cover reconstructions. Given the strong temporal variability of precipitation and streamflow data related to El Niño–Southern Oscillation (ENSO), we use Hilbert–Huang transformation to detrend the time series of streamflow and precipitation data. The adaptive data analysis is based on empirical mode decomposition techniques that are appropriate for nonlinear and nonstationary time series data (Huang et al., 1998). After empirical mode decomposition, the remaining long-term trends in streamflow and precipitation are contrasted to the observed patterns of land cover change.

The study is realised in an exceptional setting, the Pangor catchment (c. $282\,\text{km}^2$) in the Ecuadorian Andes. Situated on the Western escarpment of Ecuadorian Andes, the area is particularly affected by El Niño–Southern Oscillation cycles (Rossel, 1997). Land cover change is rapid, and resulted in a net loss of native forests and grasslands by about 20 % of the total catchment area between 1963 and 2009 (Balthazar et al., 2015). By analysing long time-series of hydrometeorological data, we specifically tested the relative sensitivity of streamflow to climate and land cover change.

2 Regional setting

The Pangor catchment (78°50′–79°01′ W, 1°43′–1°58′ S) is located at 200 km southwest of the capital of Ecuador, Quito (Fig. 1). The catchment has pronounced relief with elevation ranging between 1434 and 4333 m a.s.l. over a distance of less than 30 km. Slopes are typically steep with slope gradients around 55 %, but steeper in the dissected river valleys. The climate can be described as equatorial mesothermic semi-humid to humid (Pourrut, 1994), with precipitation and temperature increasing strongly with altitude. Mean annual precipitation at J. de Velasco station (3100 m a.s.l.; Fig. 1) is about 1400 mm (1970–2009), with high inter-annual variability ranging from 475 mm (2002) to 3700 mm (1994); whereas at Chimbo DJ Pangor station (1450 m a.s.l.) annual precipitation is only about 1000 mm (INAMHI, 2009).

The underlying geology consists of volcanic and meta-sedimentary rocks of Cretaceous to Early Tertiary age, with remnants of recent volcanic deposits at higher elevations. Soils have been classified as Andisols, Histosols and Mollisols following the USDA soil taxonomy (Gonzalez Artieda et al., 1986), and are characterised by a remarkably high water-holding capacity and soil organic matter content when undisturbed (Podwojewski et al., 2002). The landscape pattern now reflects several decades of rapid land cover change. At mid and low altitudes, a complex patchwork of small agricultural plots, remnants of sub-alpine cloud forest, and patches of abandoned land with regeneration of natural shrub vegetation can be observed. Smallholder farming is the dominant agricultural activity, and crop rotation is a common practice where annual crops are alternated with pasture. Crop species vary with altitude, with maize (*Zea mays*) grown in association with common bean (*Phaseolus vulgaris*) at altitudes below 2600 m a.s.l., and potato (*Solanum spp.*), faba bean (*Vicia faba*) and cereals (*Triticum spp.* and *Hordeum vulgare*) at higher altitudes. Large patches of montane cloud forest are only remnant on steep slopes in areas with very low accessibility. Above the natural treeline, the páramo grasslands are dominant, but plantation forests with exotic tree species (*Pinus radiata* and *Pinus patula*) now cover extensive areas (Balthazar et al., 2015).

3 Materials and methods

3.1 Land cover change detection

Land cover change for the period 1963–2009 was reconstructed based on panchromatic aerial photographs (IGM, Quito, Ecuador) and high resolution Landsat TM (15 October 1991) and ETM+ (3 November 2001, and 6 September 2009) images. A full coverage of aerial photographs at the scale of 1/60 000 was obtained for November 1963 and 1977, and land cover mapping was realized following the procedure described by Molina et al. (2012). Three Landsat scenes (1991, 2001, 2009, from the same season) with 1T level of pre-processing were acquired from the USGS archive, and images were atmospherically and topographically corrected with ATCOR3 (Balthazar et al., 2012). To support the definition of land cover classes, a WorldView II image of 2010 with a horizontal resolution of 0.5 m (PAN) and 2 m (MS) was used (Digital Globe).

A multi-source data integration method developed by Petit and Lambin (2001) was applied to reduce imprecision and inconsistency that may result from the comparison of heterogeneous datasets (Balthazar et al., 2015). Four land cover types were defined: AL: agricultural land dominated by pastures and annual crops; F: montane cloud and subalpine forests (including primary and secondary forests); P: páramo grasslands dominated by tussock grasses and dwarf shrubs, and PP: exotic forest plantations dominated by *Pinus radiata* and *patula*.

3.2 Time series of precipitation and streamflow data

Hydrometeorological data were obtained from the National Institute of Meteorology and Hydrology of Ecuador (INAMHI). Time-series of daily precipitation records are available for four meteorological stations located in or close to the Pangor catchment (J. De Velasco, Chimbo DJ Pangor, Pallatanga and Cañi-Limbe); and daily streamflow data for the Pangor AJ Chimbo gauging station (Fig. 1). The time series are appropriate for studies of long-term trends in precipitation and streamflow, as they are of good quality (data gaps $< 10\,\%$) and cover a prolonged period of time (1974 to 2008). Only during 1997 and 2003, there is a gap in the series of observed streamflow and precipitation data of more than 3 months. The multiple linear regression method described by Mora and Willems (2012) was used to fill gaps. This method estimates correlation coefficients between all pairs of hydrometeorological stations, either for the current and preceding month, and applies a multiple linear regression equation to predict missing flow or precipitation data.

Given the low density of rain gauges in the Pangor catchment, we applied the regionalization method proposed by Mora and Willems (2012) to obtain catchment-wide or areal average precipitation depths. Based on data of altitude, vegetation pattern and precipitation regime, four meteorological regions were delineated, and the closest rain gauge station was assigned to each region. Additionally, an altitude correction factor was applied based on the observed relationship between mean annual precipitation and altitude. The areal average precipitation for the entire Pangor catchment was then calculated by summing the weighted precipitation (by surface area) of the four regions, and dividing this value by the sum of the weights. The areal average daily precipitation depths, P_{d} (mm), were aggregated into monthly data for the period 1974–2008.

The time series of streamflow data (1974–2008) is based on daily water stage readings at Pangor AJ Chimbo gauging station (Fig. 1). Stage records (m) were converted into discharge records ($\mathrm{m}^3\,\mathrm{s}^{-1}$) using the stage-discharge rating curve developed by INAMHI. The discharge was then converted to daily equivalent water depth, WD_{d} (mm), to allow direct comparison with precipitation records. To condense the time series data, the daily water depths were aggregated at monthly time step. The monthly water depths were split into quick and slow flows using the hydro-statistical toolkit WETSPRO (Water Engineering Time Series PROcessing tool). This procedure is based on subflow separation techniques, and applies a generalization of the original Chapman filter. The Chapman filter assumes exponential recession for the hydrological subflows and is derived from the general equation of a low pass filter (Willems, 2009).

To assess the consistency of the hydrometeorological datasets, two simple tests were carried out following Costa et al. (2003). First, the mean annual evapotranspiration, $\overline{\mathrm{ET}_{\mathrm{yr}}}$, was estimated as the difference between the mean areal average annual precipitation, $\overline{P_{\mathrm{yr}}}$, and mean annual equivalent water depth, $\overline{\mathrm{WD}_{\mathrm{yr}}}$, for the time period 1974–2008. This first estimate of $\overline{\mathrm{ET}_{\mathrm{yr}}}$ of 1097 mm yr^{-1} or 3.0 mm d^{-1} (resulting from the subtraction of 559 mm streamflow yr^{-1} from 1656 mm precipitation yr^{-1}, 1974–2008) is consistent with published estimates of potential evapotranspiration for this region of 1000 to 1100 mm yr^{-1} by the National Institute of Meteorology and Hydrology (INAMHI, 2009). Second, the annual evapotranspiration data, $\mathrm{ET}_{\mathrm{yr}}$, are highly associated with the areal average annual precipitation depths, P_{yr} (Fig. 2), which is characteristic for tropical Andean basins (Mora and Willems, 2012). These two assessments show that the quality of the hydrometeorological data is acceptable, so that they can reliably be used for analyses of long-term trends.

3.3 Empirical mode decomposition EMD

The empirical mode decomposition (EMD), a technique developed by Huang et al. (1998), was here used to identify trends in the time series (1974–2008) of areal average monthly precipitation depths and equivalent water depths. The EMD method decomposes a given signal into a finite set of intrinsic mode function (IMFs) components and a residual or trend. The method separates non-linear oscillatory patterns of higher frequencies from those of lower frequencies, till a constant or monotonic trend is ultimately obtained (Wu and Huang, 2004). In contrast to more traditional time series analysis techniques, such as Fourier transformation and wavelet analysis, EMD is not based on linear and stationary assumptions (Huang and Wu, 2008). As such, it can be applied to nonlinear and nonstationary data series (Peel and McMahon, 2006; Brisson et al., 2015). Huang et al. (1999) demonstrated that EMD is generally successful in retrieving the physically meaningful signals hidden in time series. In some cases, however, the physically meaningful variability tends to spread into different IMFs. Wu et al. (2009) addressed this issue, referred to as the mode-mixing problem, by computing an Ensemble EMD (EEMD). The EEMD consists in introducing a perturbation in the original signal before processing it with the EMD, allowing one to exhaust all possible IMFs from the original signal. The final IMFs and residual trend are then computed as the average of their corresponding ensemble members, IMF_i. For detailed information on EEMD, we refer to Huang et al. (1998), Wu et al. (2009) and Brisson et al. (2015).

To assess the significance of the trend obtained through EMD, its variability was compared to the variability of non-significant trends. To ensure that non-significant trends have similar characteristics than the one under assessment, a 3-step method is here proposed. First, the monthly values of the observed time series, P and WD, were randomly distributed. The resulting time series features a variability similar to the observed one, but without any meaningful trend. In total, 1000 random time series were generated. Second, following the process of the EEMD, a perturbation was added to the 1000 random time series. Finally, the trend in each random time series was derived using EMD. A trend was defined to be significant if its variability is higher than the 99th percentile of the variability of the trends derived from the random signal.

3.4 Estimation of the long-term water balance

A budget approach was used to approximate the different components of the water cycle, including evaporation and transpiration (Bruijnzeel et al., 2006). First, the annual water balance for the entire catchment was approximated as:

$$P_{yr} + HP_{yr} = WD_{yr} + ET_{yr} + \Delta S \quad (1)$$

where P_{yr} is the areal average precipitation (mm yr^{-1}), HP_{yr} is the horizontal rainfall and cloud interception (mm yr^{-1}), WD_{yr} is the equivalent water depth as derived from streamflow measurements (mm yr^{-1}), ET_{yr} is the evapotranspiration (mm yr^{-1}), and ΔS is the change in soil water storage in the catchment (mm yr^{-1}. Long-term changes in soil water storage, ΔS, can be neglected, as soils are typically shallow on the Western escarpment of the Andes so that deep infiltration is limited. Horizontal rainfall, HP_{yr}, is here also considered to be negligible for the catchment-wide water balance, as additional water input from the interception of cloud water and wind-driven rain is typically constrained to the narrow(ing) belt of cloud forests (i.e. 11.6 % of the catchment area in 2009). We can then estimate the annual evapotranspiration as

$$ET_{yr} = P_{yr} - WD_{yr}. \quad (2)$$

Second, a partial water balance was established for the two ecosystems where major changes in land cover occurred (Table 1): the tropical montane cloud forest (defined as the landscape unit between 2200 and 3200 m a.s.l. originally covered by cloud forest), and páramo ecosystems (here defined as the entire landscape unit of high altitude above the continuous forest line, 3200 m a.s.l.). Land cover data were used to estimate temporal changes in partial water balance over the period 1974–2009, as the main hydrological components were parametrized based on land cover type. As the date of the land cover maps does not correspond exactly to the time series of hydrometeorological data, the land cover of 1974 and 2008 was reconstructed based on linear interpolation of existing land cover distributions. Chi-square analysis was used to analyse the significance level of the observed changes.

In the tropical montane cloud forest, the annual evapotranspiration in the cloud forests was estimated as:

$$\mathrm{ET_{yr}} = \mathrm{Et_{yr}} + \mathrm{Ei_{yr}} + \mathrm{Es_{yr}} \quad (3)$$

$$\text{with } \mathrm{Ei_{yr}} = P_{\mathrm{yr}} - (\mathrm{Tf_{yr}} + \mathrm{Sf_{yr}}) \quad (4)$$

$$\text{and } \mathrm{Et_{yr}} = (\mathrm{Tf_{yr}} + \mathrm{Sf_{yr}}) - \mathrm{WD_{yr}} \quad (5)$$

where $\mathrm{Et_{yr}}$ is the transpiration loss of dry vegetation ($\mathrm{mm\,yr^{-1}}$), $\mathrm{Ei_{yr}}$ the loss by rainfall interception of wetted vegetation ($\mathrm{mm\,yr^{-1}}$), $\mathrm{Es_{yr}}$ the evaporation from the soil surface ($\mathrm{mm\,yr^{-1}}$, negligible under dense vegetation), $\mathrm{Tf_{yr}}$ throughfall and $\mathrm{Sf_{yr}}$ stemflow ($\mathrm{mm\,yr^{-1}}$). Fleischbein et al. (2006) measured Tf and Sf for three catchments under the montane cloud forest in the southern Ecuadorian Andes. Results of Tf and Sf were on average respectively 59 and 1 % of P. P_{yr} and $\mathrm{WD_{yr}}$ are the areal average precipitation and equivalent water depth ($\mathrm{mm\,yr^{-1}}$) that were established for the entire catchment. In this study, no detailed hydrological information is available to further spatialize P_{yr} and $\mathrm{WD_{yr}}$.

For all remaining land cover types, the annual evapotranspiration was estimated using the Penman Monteith method following Buytaert et al. (2006):

$$\mathrm{ET_{yr}} = K_{\mathrm{s}} \cdot K_{\mathrm{c}} \cdot \mathrm{ET}_{o} \quad (6)$$

where K_{s} is a water stress factor, K_{c} is the crop coefficient and ET_{o} is the reference crop evapotranspiration estimated at $1000\,\mathrm{mm\,yr^{-1}}$ for the páramo ecosystem based on INAMHI (2009). Crop coefficients for natural grass vegetation and agricultural land were established for the southern Ecuadorian Andes (Buytaert et al., 2006), and K_{c} values are estimated at 0.42 for natural grassland and 0.95 for agricultural land. Pine plantations were attributed a K_{c} value of 1 based on the crop coefficient established by Allen et al. (1998) for conifers. The water stress factor, K_{s}, was set at 1, as the soil water content in páramo soils is usually above field capacity, and soils rarely undergo water stress (Buytaert et al., 2006).

4 Results

4.1 Land cover dynamics (1963–2009)

Three main land cover change trajectories can be distinguished: (1) expansion of agricultural land by about 14 % (or 39 km^2) in 46 years' time, (2) deforestation of native forests by 11 % or (or −31 km^2) corresponding to a mean rate of 67 ha yr^{-1} and (3) afforestation with exotic species in recent years by about 5 % (or 15 km^2; Table 1; Fig. 3). Over the time period 1963–2009, about 50 % of the 64 km^2 of native forests was cleared and converted to agricultural land. Small forest remnants are now scattered over steep terrain and/or in poorly accessible sites at higher elevations. Deforestation rates were highest in the 1960s, 1970s and 1980s with a net deforestation rate of 89 ha yr^{-1}, and slowed down to about 18 ha yr^{-1} for the period 1992–2009; similar to what was reported earlier for the Ecuadorian highlands (Vanacker et al., 2003; Guns and Vanacker, 2013). The pattern of afforestation stands in sharp contrast to the deforestation pattern (Fig. 3). Afforestation is mainly concentrated in the subalpine and alpine zones, and started in the early 1990s. About 2/3 of the total decrease in páramo grasslands (−23 km^2) results from exotic forest plantations, and only 1/3 from conversion to agricultural land.

4.2 Long-term trends in precipitation and streamflow (1974–2008)

The flow regime (1974–2008) largely mimics the yearly variation in precipitation, with maximum mean monthly streamflow in April (equivalent water depth of 86 mm) and low flow in September (25 mm). More than 60 % of the annual flow is concentrated in the period between February and June. Annual values of precipitation and streamflow reveal strong inter-annual variation (Fig. 4). Given the nature of hydrometeorological data in tropical Andean basins, which often display an abrupt pattern of amplitude and frequency modulation at different time scales, EEMD is an ideal method to extract physically meaningful signals. Using EEMD, the times series of monthly precipitation values and equivalent water depths were decomposed into six intrinsic mode function (IMFs 1–6) components plus the residual or trend (Fig. 5) The EEMD detrending analysis shows that the precipitation and streamflow regime changed significantly over time (Fig. 6). The EEMD analysis shows that the observed changes in streamflow (1974–2008) are not the result of long-term climate change. Despite increased precipitation, there is a remarkable decrease in streamflow (Table 1). Over the period 1974–2008, the rate of change varied through time, and two periods of change can be distinguished based on the EEMD time series analysis. Between 1974 and 1991, the monthly precipitation amounts increased sharply, while streamflow and baseflow decreased. The rate of change decreased noticeably for the period 1992–2008 (Fig. 6).

4.3 Changes in the hydrological cycle and its components

For the two periods of change that were identified based on the results from EEMD (1974–1991, 1992–2008), flow duration curves were constructed based on the daily data (Fig. 7). The mean daily water depth is about 0.4 mm lower in the period 1992–2008 compared to 1974–1991, despite an increase in the mean daily precipitation of 0.5 mm (Table 2). The largest difference is observed for low water depths, with a decrease of the Q95 and Q90 by 77 and 75 % respectively. The moderate water depths (Q10 to Q90) decreased by 24 %, and the highest ones (Q1) by 15 % only. Results of a chi-square analysis indicate that changes in mean annual precipitation, streamflow and evapotranspiration between the two periods are significant (p value < 0.005). Streamflow and evapotranspiration exhibit the largest change with −22 and +33 % respectively. Interestingly, the magnitude of increase in estimated ET is 3-fold greater than the increase in precipitation. When analysing the monthly distribution of streamflow, it is clear that the largest decrease in streamflow is observed during the dry season (JJAS), followed by the first (JFMAM) and second (minor) rainy season (OND; Fig. 8a). Similarly, the estimated mean monthly baseflow is systematically lower (3 to 11 mm) during the most recent period (Fig. 8b). During the dry season (JJAS), about 60 % of the reduction in total flow can be contributed to the strong decrease in baseflow.

5 Discussion

5.1 Changes in water balance for montane cloud forest and páramo ecosystems

Land cover dynamics observed in the Pangor catchment are characteristic for the tropical Andes, with rapid deforestation of native forests and afforestation with exotic tree species in more recent decades. Our land cover change analysis indicates that major changes occurred in the montane cloud forest and páramo ecosystems. Table 3 highlights the estimated evaporative gains and losses (hm^3) for these two ecosystems over the period 1974–2008. In montane cloud forests, there is a net reduction of annual ET by 1.1 hm^3 (corresponding to an overall ET loss of 4 mm at the catchment scale; Table 3) as a result of the conversion of 40 % of the surface area of montane cloud forest to agricultural land. This is likely to be a conservative estimate as the contribution of additional moisture from the interception of cloud water and wind-driven rain by the cloud forests is not taken into account, and might equal 5 up to 20 % of ordinary rainfall (Bruijnzeel, 2004).

On the other hand, the development of 15 km^2 of pine plantation in high alpine grasslands is estimated to have increased transpiration losses by about 8.6 hm^3 or 31 mm (Table 3). Pine forests' water use is very high compared to native páramo vegetation as result of the large total leaf surface area and deep root systems (Buytaert et al., 2007), and it largely affects the soil water storage and retention in organic-rich páramo soils (Farley et al., 2004). In addition, the conversion of ~ 6 km^2 páramo grassland to agricultural lands is expected to have further increased the transpiration losses by 3.0 hm^3 or 11 mm (Table 3). Despite high solar radiation in the tropical Andes, the water use of native plants in páramo ecosystems is very low because of the evaporative characteristics of páramo grass species. Páramo grass tussock specie can consist of up to 90 % of dead leaves, resulting in low ET values.

Partial water budgets for the montane cloud forest and páramo ecosystems suggest that the strongest changes in evaporative water losses are observed in páramo ecosystems, where progressive colonization and afforestation of high alpine grasslands leads to a strong increase in transpiration losses. As such, the reduction in evaporative losses from the conversion of montane cloud forests (−4 mm) is cancelled out by the strong increase of transpiration in the páramo ecosystems following afforestation (+31 mm) and colonization (+11 mm). The observed land cover change in montane cloud forest and páramo ecosystems is estimated to have resulted in a net loss of annual water yield by 38 mm (or 7 % of $\mathrm{WD_{yr}}$) over the period 1974–2008, mainly as consequence of increased net evapotranspiration in páramo ecosystems. This observation further points to the importance of land use planning, to minimize the potential impact of land cover change on freshwater flow regimes in the tropical Andes.

5.2 Soil hydrology following land cover conversions

Land cover conversions are often followed by a phase of intense soil degradation that further exacerbates the anthropogenic impact on surface hydrology (Hofstede et al., 2002). Soil erosion measurements based on fallout-radionuclides for the Chimbo catchment (Central Ecuadorian Andes) clearly illustrate that soil erosion rates highly depend on land cover and management (Henry et al., 2013). Erosion rates in páramo grasslands are estimated at 9 $\mathrm{t\,ha^{-1}\,yr^{-1}}$, and are significantly higher in forest plantations, pastures and croplands with erosion rates of resp. 21, 24 and 150 $\mathrm{t\,ha^{-1}\,yr^{-1}}$. The latter values are similar to soil erosion estimates for highly degraded Andean environments in southern Ecuador (Molina et al., 2008; Vanacker et al., 2014). Accelerated soil erosion has been shown to alter soil hydrological conditions, e.g. through a reduction of soil water infiltration rates and soil water retention capacity (Podwojewski et al., 2002; Molina et al., 2007). The effect of reduced soil water infiltration and retention after land cover change on the overall water balance can be inferred from the flow duration curves (Fig. 7). The increase of infrequent but very high flows combined with the strong decrease of baseflows, are a clear indication of the increasing flashiness of the Pangor River. The overall decrease of baseflows accounts for about 60 % of the reduction in total streamflow, and points to the decreased storage capacity of the Pangor basin.

6 Conclusion

Land cover dynamics observed in the Pangor catchment are characteristic for the tropical Andes, with rapid deforestation of native forests and afforestation with exotic tree species in more recent decades. Given the nature of hydrometeorological data in tropical Andean basins, which often display an abrupt pattern of amplitude and frequency modulation at different time scales, EEMD is an ideal method to extract physically meaningful signals. The EEMD analysis shows that the observed changes in streamflow (1974–2008) are not the result of long-term climate change. Despite increased precipitation, there is a remarkable decrease in streamflow that very likely results from direct anthropogenic disturbances after land cover change. Partial water budgets for the montane cloud forest and páramo ecosystems suggest that the strongest changes in evaporative water losses are observed in páramo ecosystems, where progressive colonization and afforestation of high alpine grasslands leads to a strong increase in transpiration losses. This observation further points to the importance of land use planning, to minimize the potential impact of land cover change on freshwater flow regimes in the tropical Andes.

Acknowledgements. The hydrometeorological data for this paper are available at the Instituto Nacional de Meteorologia y Hidrologia (INAMHI, Quito, Ecuador), and land use maps at simple request to the corresponding author. This research was supported by the Belgian Science Policy grant SR/00/133 FOMO. V. Vanacker was supported by a Prometeo grant No. 2014/615 funded by the Secretaría de Educación Superior de Ciencia, Tecnología e Innovación de la República del Ecuador. We thank M. Guns for field assistance, and F. Cisneros for facilitating access to laboratories and IT support at Promas and A. Van Rompaey for useful comments.

References

Allen, R. G., Pereira, L. S., Raes, D., and Smith, M.: Crop evapotranspiration, guidelines for computing crop water requirements, Irrigation and Drainage Paper 56, FAO, Rome, Italy, 1998.

Andréassian, V.: Water and forest: from historical controversy to scientific debate, J. Hydrol., 291, 1–27, 2004.

Balthazar, V., Vanacker, V., and Lambin, E.: Evaluation and parametrization of ATCOR3 topographic correction method for forest cover mapping in mountain areas, Int. J. Appl. Earth Obs., 18, 436–450, 2012.

Balthazar, V., Vanacker, V., Molina, A., and Lambin, E.: Impacts of forest cover change on ecosystem services in high Andean mountains, Ecol. Indic., 48, 63–75, 2015.

Bathurst, J. C., Iroumé, A., Cisneros, F., Fallas, J., Iturraspe, R., Gaviño Novillo, M., Urciuolo, A., de Bièvre, B., Guerrero Borges, V., Coello, C., Cisneros, P., Gayoso, J., Miranda, M., and Ramirez, M.: Forest impact on floods due to extreme rainfall and snowmelt in four Latin American environments 1: Field data analysis, J. Hydrol., 400, 281–291, 2011.

Bosch, J. M. and Hewlett, J. D.: A review of catchment experiments to determine the effect of vegetation changes on water yield and evapotranspiration, J. Hydrol., 55, 3–23, doi:10.1016/0022-1694(82)90117-2, 1982.

Bradley, R. S., Vuille, M., Diaz, H. F., and Vergara, W.: Threats to water supplies in the tropical Andes, Science, 312, 1755–1756, doi:10.1126/science.1128087, 2006.

Brisson, E., Demuzere, M., Willems, P., and van Lipzig, N. P. M.: Assessment of natural climate variability using a weather generator, Clim. Dynam., 44, 495–508, doi:10.1007/s00382-014-2122-8, 2015.

Bruhns, K. O.: Ancient South America, Cambridge University Press, Cambridge, New York, 1994.

Bruijnzeel, L. A.: Hydrology of Moist Tropical Forest and Effects of Conversion: a State of Knowledge Review, UNESCO, Paris, and Vrije Universiteit, Amsterdam, the Netherlands, 226 pp., 1990.

Bruijnzeel, L. A.: Hydrological functions of tropical forests: not seeing the soil for the trees?, Agr. Ecosyst. Environ., 104, 185–228, doi:10.1016/j.agee.2004.01.015, 2004.

Bruijnzeel, L. A., Burkard, R., Carvajal, A., Frumau, K. F. A., Köhler, L., Mulligan, M., Schellekens, J., Schmid, S., and Tobón-Marin, C.: Hydrological impacts of converting tropical montane cloud forest to pasture, with initial reference to northern Costa Rica, Final Technical Report DFID-FRP Project R7991, Vrije Universiteit, Amsterdam, and Forestry Research Programme of the UK, Department for International Development, London, 52 pp., 2006.

Buytaert, W., Iñiguez, V., Celleri, R., De Biévre, B., Wyseure, G., and Deckers, J.: Analysis of the water balance of small páramo catchments in south Ecuador, in: Environmental Role of Wetlands in Headwaters, edited by: Krecek, J. and Haigh, M., Springer, Dordrecht, the Netherlands, 271–281, 2006.

Buytaert, W., Iñiguez, V., and De Biévre, B.: The effects of afforestation and cultivation on water yield in the Andean páramo, Forest Ecol. Manage., 251, 22–30, 2007.

Costa, M. H., Botta, A., and Cardille, J. A.: Effects of large-scale changes in land cover on the discharge of the Tocantins River, southeastern Amazonia, J. Hydrol., 283, 206–217, 2003.

Farley, K. A., Kelly, E. F., and Hofstede, R. G. M.: Soil organic carbon and water retention following conversion of grasslands to pine plantations in the Ecuadorian Andes, Ecosystems, 7, 729–739, 2004.

Farley, K. A., Jobbágy, E. G., and Jackson, R. B.: Effects of afforestation on water yield: a global synthesis with implications for policy, Global Change Biol., 11, 1565–1576, 2005.

Fleischbein, K., Wilcke, W., Valarezo, C., Zech, W., and Knoblich, K.: Water budgets of three small catchments under montane forest in Ecuador: experimental and modelling approach, Hydrol. Process., 20, 2491–2507, 2006.

Gonzalez Artieda, A., Maldonado, F., and Vallejo, L.: Memoria Explicativa del Mapa General de Suelos del Ecuador, Sociedad Ecuatoriana de la Ciencia del Suelo, Quito, Ecuador, 38 pp., 1986.

Guns, M. and Vanacker, V.: Forest cover change trajectories and their impact on landslide occurrence in the tropical Andes, Environ. Earth Sci., 70, 2941–2952, 2013.

Harden, C. P.: Human impacts on headwater fluvial systems in the northern and central Andes, Geomorphology, 79, 249–263, 2006.

Henry, A., Mabit, L., Jaramillo, R. E., Cartagena, Y., and Lynch, J. P.: Land use effects on erosion and carbon storage of the Río Chimbo watershed, Ecuador, Plant Soil, 367, 477–491, 2013.

Hofstede, R. G. M., Groenendijk, J. P., Coppus, R., Fehse, J. C., and Sevink, J.: Impact of pine plantations on soils and vegetation in the Ecuadorian high Andes, Mt. Res. Dev., 22, 159–167, 2002.

Huang, N. E. and Wu, Z.: A review on Hilbert–Huang transform: method and its applications to geophysical studies, Rev. Geophys., 46, 1–23, 2008.

Title Page
Abstract | Introduction
Conclusions | References
Tables | Figures
◂◂ | ▸▸
◂ | ▸
Back | Close
Full Screen / Esc
Printer-friendly Version
Interactive Discussion

Huang, N. E., Shen, Z., Long, S. R., Wu, M. C., Shih, H. H., Zheng, Q., Yen, N.-C., Tung, C. C., and Liu, H. H.: The empirical mode decomposition and the Hilbert spectrum for nonlinear and nonstationary time series analysis, P. Roy. Soc. Lond. A, 454, 903–995, 1998.

Huang, N. E., Shen, Z., and Long, S. R.: A new view of nonlinear water waves: the Hilbert spectrum, Annu. Rev. Fluid Mech., 31, 417–457, 1999.

Instituto Nacional de Meteorología e Hidrologí a (INAMHI): Anuario Meteorológico, No. 49, Dirección de Gestión Meteorológica, Procesamiento y Edición (SIGIHM), Quito, Ecuador, 2009.

Marengo, J. A., Soares, W. R., Saulo, C., and Nicolini, M.: Climatology of the Low Level Jet east of the Andes as derived from the NCEP-NCAR reanalyses: characteristics and temporal variability, J. Climate, 17, 2261–2280, 2004.

Molina, A., Govers, G., Vanacker, V., Poesen, J., Zeelmaekers, E., and Cisneros, F.: Runoff generation in a degraded Andean ecosystem: interaction of vegetation cover and land use, Catena, 71, 357–370, 2007.

Molina, A., Govers, G., Poesen, J., Van Hemelryck, H., De Biévre, B., and Vanacker, V.: Environmental factors controlling spatial variation in sediment yield in a central Andean mountain area, Geomorphology, 98, 176–186, 2008.

Molina, A., Vanacker, V., Balthazar, V., Mora, D., and Govers, G.: Complex land cover change, water and sediment yield in a degraded Andean environment, J. Hydrol., 472–473, 25–35, 2012.

Mora, D. E. and Willems, P.: Decadal oscillations in rainfall and air temperature in the Paute River Basin–southern Andes of Ecuador, Theor. Appl. Climatol., 108, 267–282, 2012.

Nosetto, M. D., Jobbágy, E. G., and Paruelo, J. M.: Land-use change and water losses: the case of grassland afforestation across a soil textural gradient in central Argentina, Global Change Biol., 11, 1101–1117, 2005.

Peel, M. C. and McMahon, T. A.: Recent frequency component changes in interannual climate variability, Geophys. Res. Lett., 33, L16810, doi:10.1029/2006GL025670, 2006.

Petit, C. and Lambin, E. F.: Integration of multi-source remote sensing data for land cover change detection, Int. J. Geogr. Inf. Sci., 15, 785–803, 2001.

Podwojewski, P., Poulenard, J., Zambrana, T., and Hofstede, R.: Overgrazing effects on vegetation cover and volcanic ash soil properties in the páraramo of Llangahua and La Esperanza (Tungurahua, Ecuador), Soil Use Manage., 18, 45–55, 2002.

Ponette-Gonzalez, A. G., Marin-Spiotta, E., Brauman, K. A., Farley, K. A., Weathers, K. C., and Young, K. R.: Hydrologic responses in the high-elevation tropics: heterogeneous responses to land change, Bioscience, 64, 92–104, 2014.

Pourrut, P. (Ed.): Climat de l'Equateur, et l'Eau en Equateur, Principaux Acquis en Hydroclimatologie, Orstom, Instituto Francés de Investigaciones Científicas para el Desarrollo en Cooperación, Colección Estudios y Tesis, Paris, 1994.

Poveda, G. and Mesa, O. J.: Feedbacks between hydrological processes in tropical South America and large-scale ocean–atmospheric phenomena, J. Climate, 10, 2690–2702, 1997.

Restrepo, J. D. and Kjerfve, B.: Magdalena River: interannual variability (1975–1995) and revised water discharge and sediment load estimates, J. Hydrol., 235, 137–149, 2000.

Roa-García, M. C., Brown, S., Schreier, H., and Lavkulich, L. M.: The role of land use and soils in regulating water flow in small headwater catchments of the Andes, Water Resour. Res., 47, W05510, doi:10.1029/2010WR009582, 2011.

Rossel, F.: Influencia de El Niño Sobre los Régimenes Hidropluviométricos del Ecuador, Series INSEQ, vol. 18, INAMHI, Quito, 1997.

Ruprecht, J. K. and Schofield, N. J.: Analysis of streamflow generation following deforestation in southwest Western Australia, J. Hydrol., 105, 1–17, 1989.

Scott, D. F., Bruijnzeel, L. A., and Mackensen, J.: The hydrological and soil impacts of forestation in the tropics, in: Forests, Water and People in the Humid Tropics, edited by: Bonell, M. and Bruijnzeel, L. A., Cambridge University Press, Cambridge, UK, 622–651, 2005.

Tapley, T. D. and Waylen, P. R.: Spatial variability of annual precipitation and ENSO events in western Peru, Hydrolog. Sci. J., 35, 429–446, 1990.

Urrutia, R. and Vuille, M.: Climate change projections for the tropical Andes using a regional climate model: temperature and precipitation simulations for the end of the 21st century, J. Geophys. Res., 14, D02108, doi:10.1029/2008JD011021, 2009.

Vanacker, V., Govers, G., Barros, S., Poesen, J., and Deckers, J.: The effect of short-term socio-economic and demographic changes on land-use dynamics and its corresponding geomorphic response with relation to water erosion in a tropical mountainous catchment, Ecuador, Landscape Ecol., 18, 1–15, 2003.

Vanacker, V., Bellin, N., Molina, A., and Kubik, P. W.: Erosion regulation as a function of human disturbances to vegetation cover: a conceptual model, Landscape Ecol., 29, 293–309, 2014.

Vuille, M., Bradley, R. S., and Keimig, F.: Climate variability in the Andes of Ecuador and its relation to tropical Pacific and Atlantic sea surface temperatures anomalies, J. Climate, 13, 2520–2535, doi:10.1175/1520-0442, 2000.

White, S. and Maldonado, F.: The use and conservation of national resources in the Andes of southern Ecuador, Mt. Res. Dev., 11, 37–55, 1991.

Willems, P.: A time series tool to support the multi-criteria performance evaluation of rainfall–runoff models, Environ. Modell. Softw., 24, 311–321, 2009.

Wu, Z. and Huang, N. E.: A study of the characteristics of white noise using the empirical mode decomposition method, P. Roy. Soc. Lond. A, 460, 1597–1611, 2004.

Wu, Z. and Huang, N. E.: Ensemble empirical mode decomposition: a noise-assisted data analysis method, Adv. Adapt. Data Anal., 01, 1–41, doi:10.1142/S1793536909000047, 2009.

Table 1. Proportions (in percent) of the four land cover types for 1963, 1977, 1991, 2001 and 2009, and amount of land cover change for period 1963–2009 as percentage of the catchment surface area (%).

Land cover type	1963	1977	1991	2001	2009	Δ (1963–2009)
Agricultural land (AL)	33.6	39.0	45.3	46.5	47.4	+13.8
Native forest (F)	22.5	18.5	13.8	12.8	11.6	−10.9
Páramo grassland (P)	43.9	42.5	40.5	37.4	35.7	−8.2
Exotic forest plantation (PP)	0.0	0.0	0.4	3.3	5.3	+5.3

Table 2. Long-term mean of the main surface hydrological components. $\overline{P_\mathrm{d}}$ is the mean daily precipitation and $\overline{\mathrm{WD}_\mathrm{d}}$ the mean daily water depth derived from the hydrometeorological dataset for the periods 1974–1991 and 1992–2008. $\overline{\mathrm{ET}_\mathrm{d}}$ is the mean daily evapotranspiration, estimated following Eq. (2). All hydrological components are expressed in mm.

Period	$\overline{P_\mathrm{d}}$ (mm)	$\overline{\mathrm{WD}_\mathrm{d}}$ (mm)	$\overline{\mathrm{ET}_\mathrm{d}}$ (mm)
1974–1991	4.3	1.7	2.6
1992–2008	4.8	1.3	3.5

Table 3. Evaporative gains and losses over the period 1974–2008 in (a) montane forest and (b) páramo ecosystems. ET_{past} corresponds to the evaporative losses of the land units prior land cover change, ET to the evaporative losses after land cover change and ΔET to the overall change in evaporation due to land cover change during the period 1974–2008. The ET values are expressed in hm^3 to indicate the changes in partial water budgets for the land units undergoing land cover change. To allow direct comparison with the results from the long-term time series analyses at the catchment scale, ΔET is also expressed in mm by dividing the estimated water production of the land units (hm^3) by the total catchment area (km^2) and one thousand to convert the values to mm.

	Conversion from...	Area (km^2)	ET_{past} (hm^3)	ET (hm^3)	ΔET (hm^3)	ΔET (mm)
(a)	Native forest to agricultural land	21.4	23.5	22.4	−1.1	−4
(b)	Páramo grassland to agriculture	5.7	2.4	5.4	+3.0	+11
	Páramo grassland to plantations	14.9	6.3	14.9	+8.6	+31

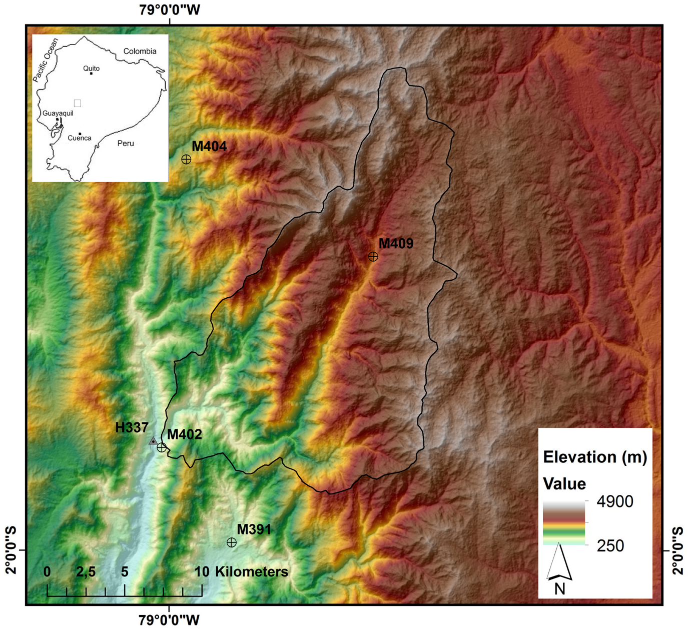

Figure 1. Location map of the Pangor catchment on the western escarpment of the Ecuadorian Andes. The ASTER GDEM V2 30 m resolution digital elevation model was draped over the hillshade model. The location of the gauging station (H337, Pangor AJ Chimbo) is shown with a triangle, and the rain gauges (M402: Chimbo DJ Pangor, M404: Cani-Limbe; M409: J. de Velasco, M391: Pallatanga) with a black cross. The inset map at the upper left shows the location of the study area within South America.

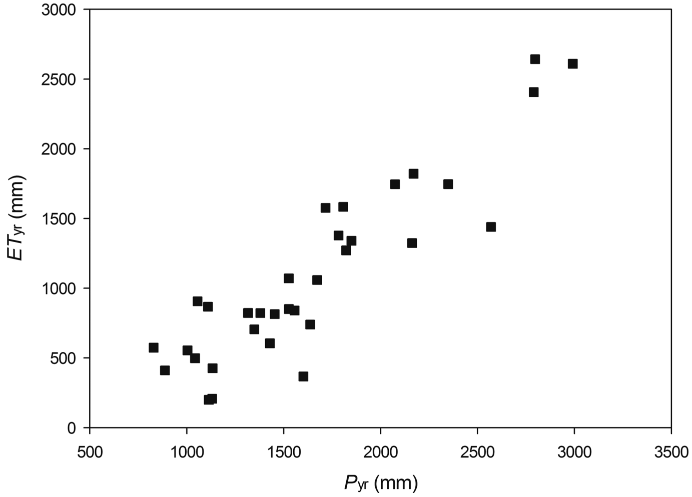

Figure 2. Scatterplot between areal average annual precipitation P_{yr} and annual evapotranspiration ET_{yr}.

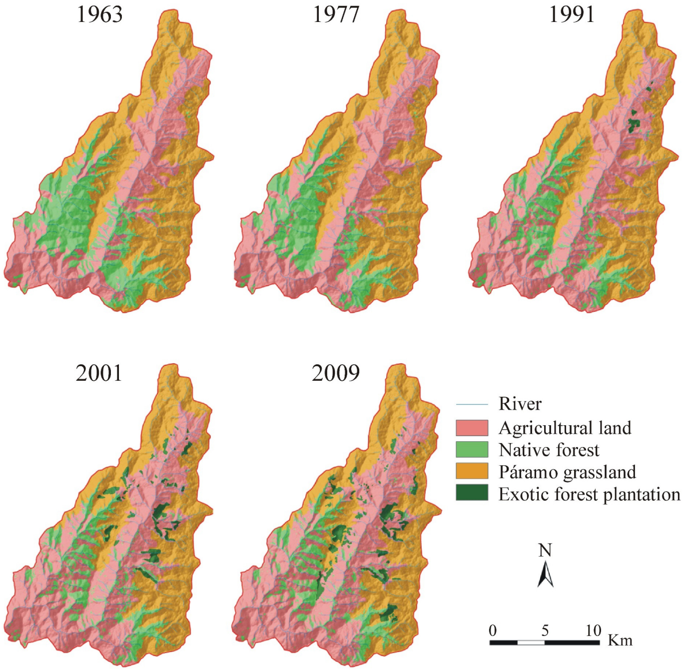

Figure 3. Land cover maps of 1963, 1977, 1991, 2001 and 2009 based on panchromatic aerial photographs and high resolution Landsat images. Four land cover types were identified: agricultural land, montane cloud and subalpine forests, paramo grasslands and exotic forest plantations.

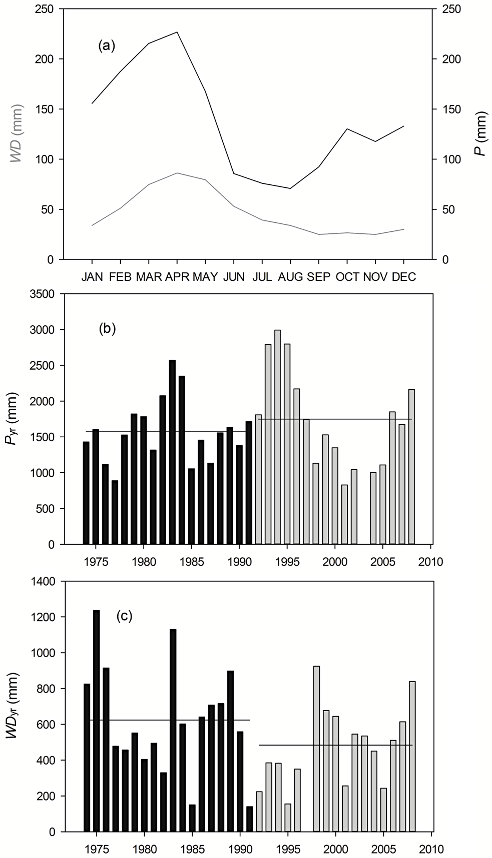

Figure 4. Hydrological characteristics of the study area. **(a)** Mean monthly streamflow (gray line, left *y* axis) and average monthly rainfall (black line, right *y* axis) for the period 1974–2008, **(b)** time series of areal average annual precipitation and **(c)** equivalent water depth.

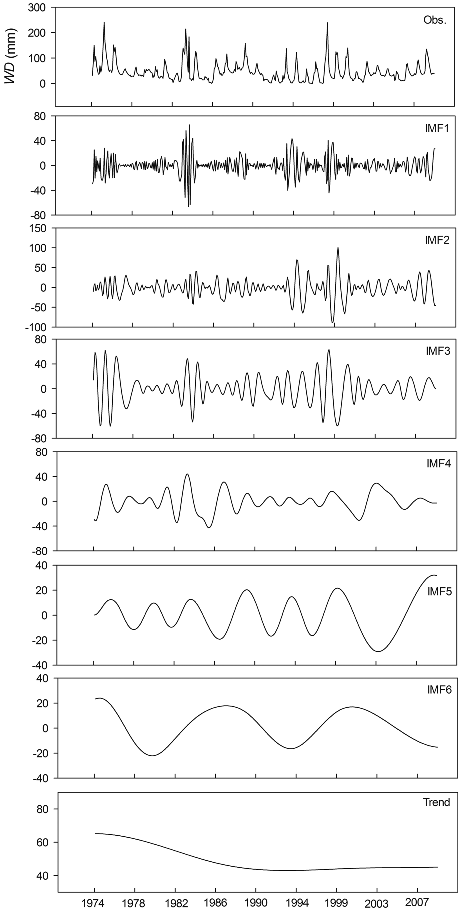

Figure 5. EEMD analysis of time series (1974–2008) of monthly water depths, with observed mean monthly streamflow (top panel), the six corresponding intrinsic mode functions and the monotonous trend or residual (bottom panel).

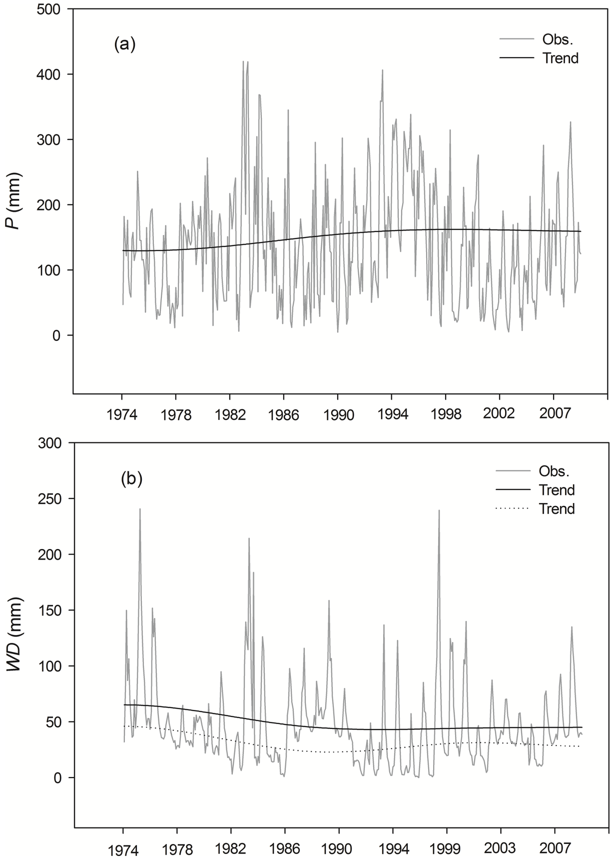

Figure 6. Residuals or trends in rainfall, streamflow and baseflow following EEMD time series analysis (1974–2008). **(a)** Observed areal average monthly rainfall (grey line) and residual trend (black line). **(b)** Observed monthly equivalent water depth (grey line) and residual trend in streamflow (continuous black line) and baseflow (dotted black line).

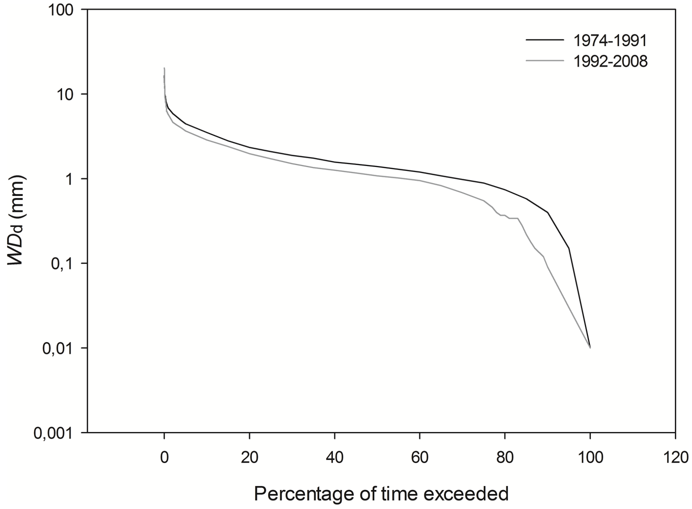

Figure 7. Flow duration curves for the period 1974–1991 (black line) and 1992–2008 (grey line).

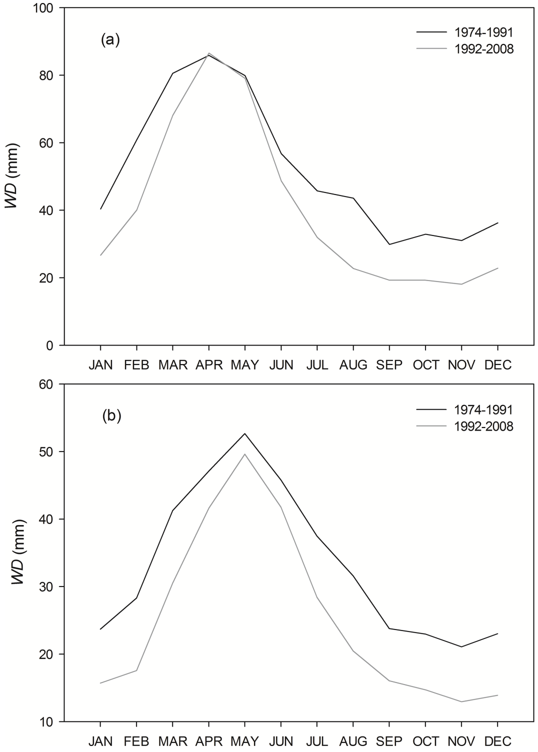

Figure 8. (a) Mean monthly streamflow and **(b)** mean monthly baseflow for period 1974–1991 (black line) and 1992–2008 (grey line).